Line Outage Detection Using Phasor Angle Measurements

Joseph Euzebe Tate, *Member, IEEE*, and Thomas J. Overbye, *Fellow, IEEE*

***Abstract*—Although phasor measurement units (PMUs) have become increasingly widespread throughout power networks, the buses monitored by PMUs still constitute a very small percentage of the total number of system buses. Our research explores methods to derive useful information from PMU data in spite of this limited coverage. In particular, we have developed an algorithm which uses known system topology information, together with PMU phasor angle measurements, to detect system line outages. In addition to determining the outaged line, the algorithm also provides an estimate of the pre-outage flow on the outaged line. To demonstrate the effectiveness of our approach, the algorithm is demonstrated using simulated and real PMU data from two systems—a 37-bus study case and the TVA control area.**

***Index Terms*—Event detection, line outages, phasor measurement units.**

I. Introduction

With the increasing loading of the power system, along with the massive interarea transfers enabled by the deregulation of the 1980s and 1990s, there is a clear need to have reliable information about both the local system and external systems. Tellingly, four of the six major North American blackouts were due in part to a lack of situational awareness [1]. Although there is a clear need for sharing of information, there is limited real-time sharing of SCADA or state estimator information in the United States [2]. However, as phasor measurement units (PMUs) [3] have been deployed throughout the North American power grid, there have been significant efforts to ensure that PMU data are shared between all interested parties [4]. Because PMU data are more widely available in near real-time than other power system measurement data, it can provide unique insights into the global operation of the grid. However, new techniques must be developed to apply the data that PMUs provide in a useful manner.

Extensive research in applying PMU information to improve situational awareness has been conducted since their introduction, including applications in state estimation [5]–[7], dynamic security assessment [8]–[10], and visualization [11]–[13]. Yet another key aspect of situational awareness in the power grid is the knowledge of transmission line, transformer, and generator statuses. Beyond incorporation of PMUs into traditional state estimation, which can include topology estimation [14], there has been little research into how PMUs can be used to enhance topology information, particularly outside of the local area. Current network topology processors focus on obtaining local system topology information through the use of predominantly local area measurements [15]–[18]. However, connectivity information over the wide area is very important for system operations and is a major reason for the existence of the NERC System Data Exchange (SDX) [19]. Because there is significant value in improving system operators' knowledge of external system line outages, we have developed a method which utilizes PMU data to effect this improvement.

Our method makes extensive use of SDX information, as it is currently the best source of system-wide line status information. One of the most telling indications of its usefulness is its application in processing transmission loading reliefs (TLRs) on the North American power grid. However, despite increased awareness of the importance of interarea information exchange since the August 2003 blackout, updates to the SDX are still only required on an hourly basis [20]. Because much can happen on the power grid within an hour, there is a need for tools which are capable of providing more current information on external system outages. Our work looks at ways to improve upon the status information from local topology processors and the NERC SDX by incorporating PMU data which, like SDX information, is also available over the entire interconnect through phasor data concentrators (PDCs) [4]. The method presented here is one possible application in which pre-outage topology information from the NERC SDX is combined with real-time PMU angle measurements to detect single line outages on the system. Although the methods presented here would work with any source of synchronized angle data, PMUs are the only devices which are deployed over the entire power grid and are capable of providing geographically dispersed, synchronized, and accurate phasor angle measurements.

II. Problem Formulation

The problem addressed in this work is the detection of single line outages using only PMU data, transmission line and transformer parameter data, and system topology information. One key assumption made is that the fast system dynamics are well-damped and that the system settles down into a quasi-stable state following the line outage. We account for the possibility of poor damping of slower, electromechanical oscillations through the

Manuscript received November 26, 2007; revised April 02, 2008. Current version published October 22, 2008. This work was supported in part by the U.S. National Science Foundation (NSF) awards 0540237 and 0524695, in part by the Power Systems Engineering Research Center, and in part by an NSF Graduate Research Fellowship. Data were also provided by the Tennessee Valley Authority for evaluation of our algorithm. Paper no. TPWRS-00864-2007.

J. E. Tate is with the Department of Electrical and Computer Engineering, University of Toronto, Toronto, ON M5S 3G4 Canada (e-mail: zeb.tate@utoronto.ca).

T. J. Overbye is with the Department of Electrical and Computer Engineering, University of Illinois at Urbana-Champaign, Urbana, IL 61801 USA (e-mail: overbye@uiuc.edu).

Color versions of one or more of the figures in this paper are available online at http://ieeexplore.ieee.org.

Digital Object Identifier 10.1109/TPWRS.2008.2004826

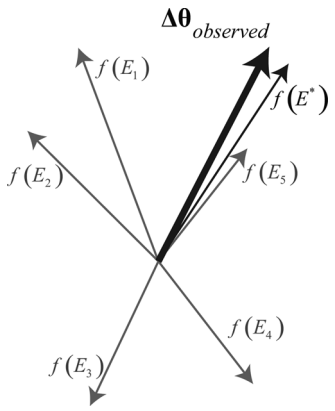

Fig. 1. Determining the event which best matches the observed angle changes.

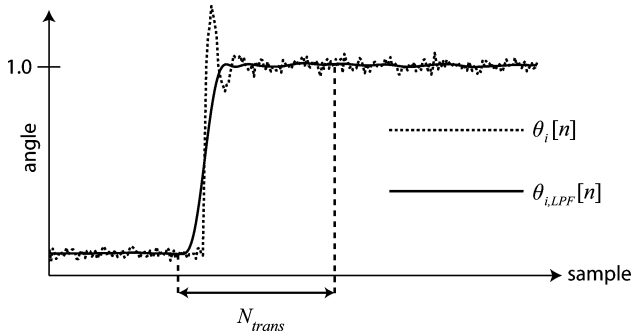

Fig. 2. Low-pass filtering of phasor angle measurements with noise and oscillations.

use of low-pass filtering, as discussed below. Furthermore, although the power flow solutions to the system before and after the event do not take into account system dynamics, it is assumed that the power flow solution after the event will closely match the system values measured after the system oscillations have damped out [21] or been filtered out.

Following a system event, the phasor angle differences at the observable buses in the system with respect to their pre-event values can be determined. Once the changes in angles at each bus has been determined (denoted as the K-dimensional vector $\boldsymbol{\Delta\theta}_{observed}$, where K is the number of phasor angles observable using PMUs), the following optimization problem is solved:

$$E^* = \arg\min_{E\in\mathcal{E}} ||\boldsymbol{\Delta\theta}_{observed} - f(E)|| \tag{1}$$

where $\mathcal{E}$ is the set of events to be checked for occurrence, and $f(E)$ is a function which relates an event E to the changes in angles caused by the event. Fig. 1 provides a visual depiction of (1), although (1) is K-dimensional while the figure is only two-dimensional. In this figure, the changes in angles due to the nonminimizing events, $f(E_{1-5})$, are colored gray and the angle change vector from the best matching event, $f(E^*)$, is shown in black.

III. Detecting Event Occurrence and Extracting Angle Changes

A. Event Detection and Angle Extraction Methodology

In order to evaluate the possibility of an event having occurred on the system, it is first necessary to determine the quasi-steady state changes in measured phasor angles, $\boldsymbol{\Delta\theta}_{observed}$. The phasor angle measurements at bus i are referred to as $\theta_i[n]$, where n is the nth sample of the phasor angle. Because only the quasi-steady state angle values are of interest, rather than the total dynamic response, any fast oscillations in the phasor angles must be filtered out, along with any other noise present in the measurement signals. Therefore, the original angle measurements are filtered with a low-pass filter having a cutoff frequency of 0.2 Hz; the output of this filter is named $\theta_{i,LPF}[n]$ for the phasor angle measurements at bus i. An example measurement, along with the low-pass filtered form of the measurement, is given in Fig. 2. This is the same filter method used to show PMU data in [22] and is needed to attenuate oscillations which may be present after the event occurs. As shown in Fig. 2, the filter eliminates much of the noise in the signal and also the 0.5–3 Hz oscillations typically seen after a line outage. Once the phasor angles have been low-pass filtered, a candidate angle change signal $\Delta\theta_{i,candidate}[n]$ is constructed for each bus i, as follows:

$$\Delta\theta_{i,candidate}[n] = \theta_{i,LPF}[n] - \theta_{i,LPF}[n - N_{trans}] \tag{2}$$

where N_{trans} is the number of samples over which a difference in steady state angles is calculated (see Fig. 2).

To detect whether an event has occurred, a method commonly used in edge detection [23] was adapted for our purposes. To detect when an event has occurred, each of the candidate signals $|\Delta\theta_{i,candidate}[n]|$ is continuously compared against a threshold value τ. If the candidate signal at bus j exceeds the threshold value at sample $n_{initial}$, candidate signal $|\Delta\theta_{j,candidate}[n]|$ is then tracked for $n > n_{initial}$ until it begins to decrease. A decrease implies that the maximum of $|\Delta\theta_{j,candidate}[n]|$ has been reached, and the $\boldsymbol{\Delta\theta}_{observed}$ vector is then constructed using the angle information from all of the buses.

The pseudocode for this "hill climbing" procedure, visualized in Fig. 3, is

$$\begin{aligned}
&\text{if } |\Delta\theta_{j,candidate}[n_{initial}]| > \tau \text{ for a bus } j,\\
&n_{\max} \leftarrow n_{initial}\\
&\Delta^2\theta_{j,candidate} \leftarrow +\infty\\
&\Lambda \leftarrow \text{sign}\left(\Delta\theta_{j,candidate}[n_{\max}]\right)\\
&\text{while } \left(\Delta^2\theta_{j,candidate} \geq -\gamma\right)\\
&\quad \Delta^2\theta_{j,candidate} \leftarrow \Big(\Delta\theta_{j,candidate}[n_{\max}+1]\\
&\qquad - \Delta\theta_{j,candidate}[n_{\max}]\Big)\\
&\quad \text{if } \left(\Lambda \times \Delta^2\theta_{j,candidate} > 0\right) \text{ then } n_{\max} \leftarrow n_{\max} + 1
\end{aligned} \tag{3}$$

where γ is a parameter which allows for small decreases in the midst of continuing increases when determining where the maximum value of $|\Delta\theta_{j,candidate}[n]|$ occurs. After $n_{\max}$ has been determined according to (3) using the angle information

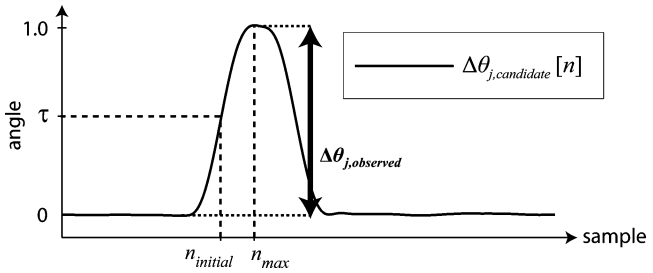

Fig. 3. Peak detection and determination of the observed angle change vector.

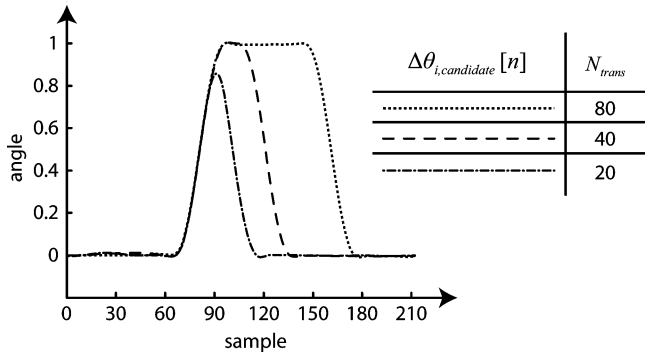

Fig. 4. Effect of N_{trans} selection on $\Delta\theta_{i,candidate}[n]$ signal.

from bus j, the observed angle change vector is then constructed using the sample from all of the candidate signals, as follows:

$$\Delta\boldsymbol{\theta}_{observed} = \begin{bmatrix} \Delta\theta_{1,candidate}[n_{\max}] \\ \Delta\theta_{2,candidate}[n_{\max}] \\ \vdots \\ \Delta\theta_{K,candidate}[n_{\max}] \end{bmatrix}. \quad (4)$$

B. Parameter Selection

There are three key parameters involved in both the event detection and angle change vector extraction as formulated in the previous section: N_{trans}, τ, and γ. The first of these parameters, N_{trans}, is the number of samples over which the difference in angle measurements is taken. N_{trans} must be large enough for the entire transition region to fit inside N_{trans} samples, otherwise the resulting $\Delta\theta_{i,candidate}[n]$ signal will underestimate the true difference in steady state angle values. On the other hand, choosing a value of N_{trans} which is excessively large will cause a longer wait time before the $\Delta^2\theta_{i,candidate} < \gamma$ condition is met. Fig. 4 illustrates how varying N_{trans} from 20 to 80 affects the $\Delta\theta_{i,candidate}$ signal obtained from the $\theta_{i,LPF}$ signal in Fig. 3. Using an N_{trans} value of 20 samples results in underestimation of the angle change to approximately 0.8, whereas using a value of 80 samples requires a delay of more than 60 samples relative to the $N_{trans} = 40$ case before the $\Delta^2\theta_{i,candidate} < \gamma$ condition is met.

The threshold value τ must be chosen with care, because setting the threshold value too high might result in missing events that only result in small angle changes (e.g., outage of lines with low pre-outage flow), whereas choosing a threshold value which is too low could result in misclassification of noise as an event. Based on the IEEE standard governing PMU behavior [24], a threshold of 0.57 degrees was used to avoid misclassification of noise as an event. This results in a classification scheme which results in more false negatives than false positives, with the understanding that the results might be used to alarm operators to system changes.

The third parameter, γ, is used to ensure that $n_{\max}$ is determined correctly once the angle differences have exceeded the threshold level. For the examples shown below, γ was set to 10% of the threshold value τ (i.e., 0.057 degrees). This value was chosen based on analysis of real and simulated PMU measurements after events and could be reduced if a filter is used which better eliminates overshoot.

IV. Single Line Outage Detection Algorithm

A. Analytical Basis for Line Outage Detection Using Quasi-Steady State Angle Changes

When ξ is restricted to a set of single line outages on the system, then the problem defined in (1) becomes

$$\text{line outaged } l^* = \underset{l\in\{1,2,\ldots,L\}}{\arg\min}\left(\min_{P_l}\|\Delta\boldsymbol{\theta}_{observed} - deltaAngles_l(P_l)\|\right) \quad (5)$$

where L is the number of lines in service before the event is detected and $deltaAngles_l(P_l)$ is the calculated change in angles that would occur for a pre-outage flow of P_l on line l. Because P_l is allowed to vary in order to achieve the best match in observed and calculated angles, a unique solution of (5) requires that each line outage be distinguishable from the outage of other lines regardless of the pre-outage flow on each line.

Solution of (5) requires the ability to relate the pre-outage flow on a line l to the observed angle changes on that line if it were to be outaged (represented by $deltaAngles_l(P_l)$). A simple expression for $deltaAngles_l(P_l)$ is obtained if the dc power flow equations are used. Consider the following relationship between changes in power injections and angles based on the dc power flow assumptions:

$$\Delta\boldsymbol{\theta} = \mathbf{B}^{-1}\Delta\mathbf{P} \quad (6)$$

where $\Delta\boldsymbol{\theta}$ is the changes in angles at all system buses due to a change in power injections of $\Delta\mathbf{P}$. The $\mathbf{B}$ matrix used here can be determined using line status information from a source of system-wide topology data (e.g., the NERC SDX).

When the dc power flow equations are used, the effect of the outage of a line l can be approximated by a power transfer between the line's "to" bus l_{to} and its "from" bus l_{from}[25]. The transfer amount $\tilde{P}_l$ can be determined from the following equation:

$$\tilde{P}_l = \frac{-P_l}{1 + PTDF_{l,l_{\text{to}}-l_{\text{from}}}} \quad (7)$$

where P_l is the pre-outage flow on line l defined as positive if flowing from l_{from} to l_{to}. The value $PTDF_{l,l_{\text{to}}-l_{\text{from}}}$ is the power transfer distribution factor (PTDF) relating the change in flow on line l due to a transfer from l_{to} to l_{from} , and can be calculated using only topology and impedance information if the dc power flow assumptions are used [26].

If the power injection $\tilde{P}_l$ is imposed on the system, then a change in angles occurs at all buses. To distinguish the observable angles from the complete set of angles at all buses, a K by N matrix $\mathbf{K}$ is introduced, as follows:

$$\mathbf{K} = [\,\mathbf{I}_{K\times K} \quad \mathbf{0}_{K\times(N-K)}\,] \tag{8}$$

where K is the number of phasor angles observable from the PMUs, N is the total number of system buses, $\mathbf{I}_{K\times K}$ is the $K\times K$ identity matrix, and $\mathbf{0}_{K\times(N-K)}$ is a $K\times(N-K)$ matrix of zeros. The set of angle changes at the observable buses, which is denoted as $\Delta\boldsymbol{\theta}^{\tilde{P}_l}_{calc,l}$, is then found by applying (6), as follows:

$$\begin{aligned}\Delta\boldsymbol{\theta}^{\tilde{P}_l}_{calc,l} &= \mathbf{K}\mathbf{B}^{-1}\begin{bmatrix}0\\ \tilde{P}_l\\ -\tilde{P}_l\\ 0\end{bmatrix}\begin{matrix}\\ \leftarrow l_{\text{to}}\\ \leftarrow l_{\text{from}}\\ \\ \end{matrix}\\ &= \tilde{P}_l\mathbf{K}\mathbf{B}^{-1}\begin{bmatrix}0\\ 1\\ -1\\ 0\end{bmatrix}\begin{matrix}\\ \leftarrow l_{\text{to}}\\ \leftarrow l_{\text{from}}\\ \\ \end{matrix}\\ &= \tilde{P}_l\Delta\tilde{\boldsymbol{\theta}}_{calc,l}.\end{aligned} \tag{9}$$

As shown in (9), the changes in angles are linear with respect to $\tilde{P}_l$; therefore, the calculated changes in angles for a particular pre-outage flow on line l can be written as a scalar $\tilde{P}_l$ multiplying a constant vector $\Delta\tilde{\boldsymbol{\theta}}_{calc,l}$. In turn, (5) can be rewritten with $deltaAngles_l(P_l)$ replaced by the appropriate scalar-vector product, as follows:

$$\begin{aligned}&\text{line outaged } l^*\\ &\quad= \underset{l\in\{1,2,\ldots,L\}}{\arg\min}\left(\min_{\tilde{P}_l}\left\|\Delta\boldsymbol{\theta}_{\text{observed}} - \tilde{P}_l\Delta\tilde{\boldsymbol{\theta}}_{calc,l}\right\|\right).\end{aligned} \tag{10}$$

The optimization given in (10) can be performed very quickly using dot products. To see why this is the case, consider two vectors $\mathbf{a}$ and $\mathbf{b}$. From linear algebra, it is known that the projection of $\mathbf{b}$ onto $\mathbf{a}$, $proj_{\mathbf{a}}\mathbf{b}$, is the vector that minimizes $\mathbf{b}-k\mathbf{a}$, where k is allowed to take on any value [27]. The formula for calculating $proj_{\mathbf{a}}\mathbf{b}$ is

$$\begin{aligned}k^* &= \frac{\mathbf{a}\cdot\mathbf{b}}{\mathbf{a}\cdot\mathbf{a}} = \underset{k}{\arg\min}\|\mathbf{b}-k\mathbf{a}\|\\ proj_{\mathbf{a}}\mathbf{b} &= k^*\mathbf{a}.\end{aligned} \tag{11}$$

Comparing (10) and (11), the inner minimization of (10) can be rewritten as (12) at the bottom of the page. The inner minimization can then be eliminated and the complete minimization rewritten using dot products in (13) at the bottom of the page.

Because $\Delta\boldsymbol{\theta}_{\text{observed}}$ is a fixed vector and $\Delta\tilde{\boldsymbol{\theta}}_{calc,l}$ is scaled by the optimal value to minimize the differences in observed and calculated angle changes, the closeness of fit between the changes in angles due to the outage of line l and the observed angle changes is due to the direction associated with each vector. To quantify this relationship, a normalized angle distance metric for a given line l, NAD_l, is defined as follows:

$$NAD_l = \min\left\{\left\|\frac{\Delta\boldsymbol{\theta}_{\text{observed}}}{\|\Delta\boldsymbol{\theta}_{\text{observed}}\|} - \frac{\Delta\tilde{\boldsymbol{\theta}}_{calc,l}}{\|\Delta\tilde{\boldsymbol{\theta}}_{calc,l}\|}\right\|, \left\|\frac{\Delta\boldsymbol{\theta}_{\text{observed}}}{\|\Delta\boldsymbol{\theta}_{\text{observed}}\|} + \frac{\Delta\tilde{\boldsymbol{\theta}}_{calc,l}}{\|\Delta\tilde{\boldsymbol{\theta}}_{calc,l}\|}\right\|\right\}. \tag{14}$$

Fig. 5 shows the NAD metric and how it relates to the normalized observed and calculated angle changes. As shown in the figure, the closer the direction of the observed and expected angle change vectors, the closer the NAD value should be to zero. The minimization in the definition is needed to account for the fact that $\tilde{P}_l^*$ can be either positive or negative.

B. Basic Algorithm Definition

In order to detect a line outage, identify the outaged line, and determine the pre-outage flow on that line, the following basic algorithm is used.

1) Determine whether an outage has occurred by filtering the phasor angles and checking for a change in angles greater

$$\begin{aligned}\tilde{P}_l{}^* &= \frac{\Delta\boldsymbol{\theta}_{\text{observed}}\cdot\Delta\tilde{\boldsymbol{\theta}}_{calc,l}}{\Delta\tilde{\boldsymbol{\theta}}_{calc,l}\cdot\Delta\tilde{\boldsymbol{\theta}}_{calc,l}}\\ \min_{\tilde{P}_l}\left\|\Delta\boldsymbol{\theta}_{\text{observed}} - \tilde{P}_l\Delta\tilde{\boldsymbol{\theta}}_{calc,l}\right\| &= \left\|\Delta\boldsymbol{\theta}_{\text{observed}} - \tilde{P}_l{}^*\Delta\tilde{\boldsymbol{\theta}}_{calc,l}\right\|\end{aligned} \tag{12}$$

$$\text{line outaged } l^* = \underset{l\in\{1,2,\ldots,L\}}{\arg\min}\left(\left\|\Delta\boldsymbol{\theta}_{\text{observed}} - \left(\frac{\Delta\boldsymbol{\theta}_{\text{observed}}\cdot\Delta\tilde{\boldsymbol{\theta}}_{calc,l}}{\Delta\tilde{\boldsymbol{\theta}}_{calc,l}\cdot\Delta\tilde{\boldsymbol{\theta}}_{calc,l}}\right)\Delta\tilde{\boldsymbol{\theta}}_{calc,l}\right\|\right) \tag{13}$$

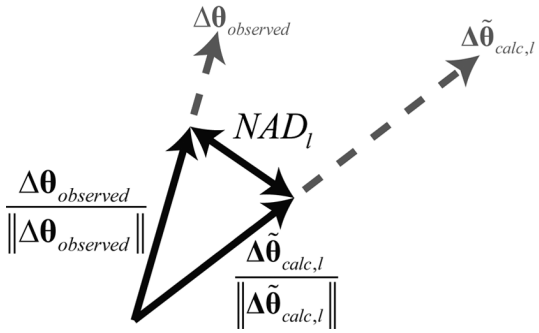

Fig. 5. Normalized angle difference (NAD) metric.

than or equal to τ. When a qualifying change is detected, proceed to step 2.

2) Determine the observed angle change vector $\boldsymbol{\Delta\theta}_{observed}$ using (3) and (4).
3) For each line l
   a) Calculate $\boldsymbol{\Delta\tilde{\theta}}_{calc,l}$ using (9).
   b) Calculate $\tilde{P}_l^*$ using (12).
   c) Calculate the NAD value for line l using (14) and the results from steps 2) and 3a), then store the calculated error value in the indexed array $NADVals$, as follows:

$$NADVals_l = NAD_l. \tag{15}$$

4) Determine the line l^* that was outaged by sorting $NADVals$, as follows:

$$l^* = \arg\min_l NADVals_l. \tag{16}$$

5) Determine the pre-outage flow on the line which best fits the observed angle, P_l^*, using (7) and the results from step 3b), as follows:

$$P_{l^*}^* = \tilde{P}_{l^*}^* \left(1 + PTDF_{l^*,l_{\text{to}}^*-l_{\text{from}}^*}\right). \tag{17}$$

C. Computational Complexity

To calculate the angle change due to the outage of a line l using (9), the $\mathbf{B}$ matrix must be factored using LU decomposition [28]. This is the most expensive operation in the algorithm, but it only needs to be performed once per change in topology. Once $\mathbf{B}$ is factored, $\boldsymbol{\Delta\tilde{\theta}}_{calc,l}$ and the necessary PTDF values can be computed using forward and backward substitution. Outside of step 3a), the algorithm requires only addition and dot products with vectors of dimension K and a sort operation. These last operations are highly parallelizable and would see performance gains on the order of the number of computing cores available.

D. Algorithm Issues

The algorithm as defined in the above section is subject to several possible errors. First, the conditions under which the dc power flow equations hold (low impedance lines, small angle differences across lines, and near-nominal voltages) are necessary in order to treat the power system as a linear system. Because in a real system these conditions are never completely satisfied, error is introduced into the calculation of $\boldsymbol{\Delta\tilde{\theta}}_{calc,l}$ and $\tilde{P}_l^*$ [29]. As a result, the calculated error values from (15) may not accurately reflect the true relationship between the outage of line l and the observed angle changes, which could lead to inaccurate line rankings.

Another possible error source is in the determination of $\boldsymbol{\Delta\theta}_{\text{observed}}$. Ideally, $\boldsymbol{\Delta\theta}_{\text{observed}}$ would correspond precisely to the quasi-steady state angle changes due to the line outage. However, errors in $\boldsymbol{\Delta\theta}_{\text{observed}}$ can be caused by inaccurate instrument transformers, analog-to-digital conversion, and the determination of $\boldsymbol{\Delta\theta}_{\text{observed}}$ based on (3) and (4).

Still another possible problem arises when multiple lines cause similar changes in phasor angles at the observed buses. Because optimal scaling is performed on the $\boldsymbol{\Delta\tilde{\theta}}_{calc,l}$ vectors, any lines a and b such that the normalized dot product is close to 1, i.e.,

$$\left| \frac{\boldsymbol{\Delta\tilde{\theta}}_{calc,a}}{\left\|\boldsymbol{\Delta\tilde{\theta}}_{calc,a}\right\|} \cdot \frac{\boldsymbol{\Delta\tilde{\theta}}_{calc,b}}{\left\|\boldsymbol{\Delta\tilde{\theta}}_{calc,b}\right\|} \right| \approx 1 \tag{18}$$

are difficult to distinguish. One obvious example where (18) would be true is if the lines a and b are parallel lines in the system. Although the case of parallel lines being indistinguishable is unavoidable, if (18) holds for nonparallel lines, then PMUs can be added to the system in order to ensure that line outages are distinguishable.

One final issue is that changes in angles on the system may be due to other types of events, such as generator outages or multiple line outages. Although we currently restrict $\mathcal{E}$ to consist of all possible single line outages, other types of events could be considered using the basic formulation given in (1). This would require an expansion of the set $\mathcal{E}$ and a method of determining the expected angle changes due to each event. Prior research in generalized line outage distribution factors [30] and generation shift factors [25] indicates that this determination is feasible, and, as mentioned in the conclusion below, expansion of the event set would be a useful area of future research. The inability of the algorithm to accurately detect other types of system events can also be addressed by modifying the algorithm so that a minimum NAD value is needed to classify the event as a line outage. This modification, along with several other useful modifications to the algorithm, is discussed in the next section.

E. Algorithm With Heuristics and Extended Reporting

Considering these complicating factors, modifications were made to the algorithm to aid in correct detection of a single line outage. The first modification addresses the possibility that no single line outage is responsible for the observed angle changes. This is handled by defining a minimum allowable NAD value and insuring that any reported outages have an NAD value below this threshold (i.e., in step 4, the algorithm only reports a line outage if $NADVals_{l^*}$ is below the threshold). If no outages result in a sufficiently low NAD value, the algorithm reports that the event is unidentifiable as a single line outage.

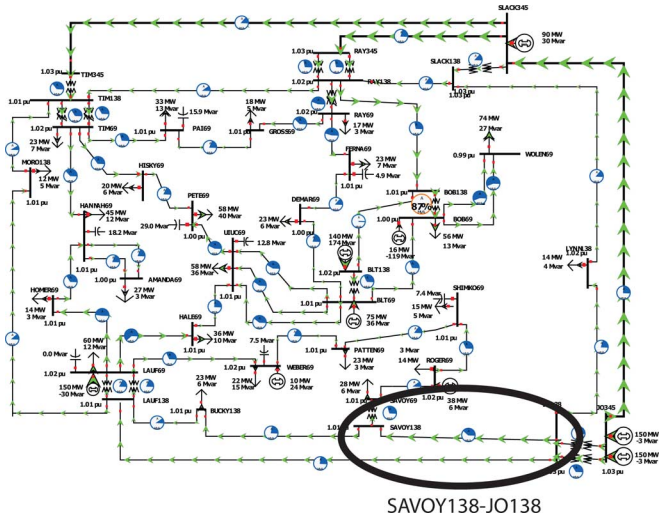

Fig. 6. Oneline diagram of 37-bus study system.

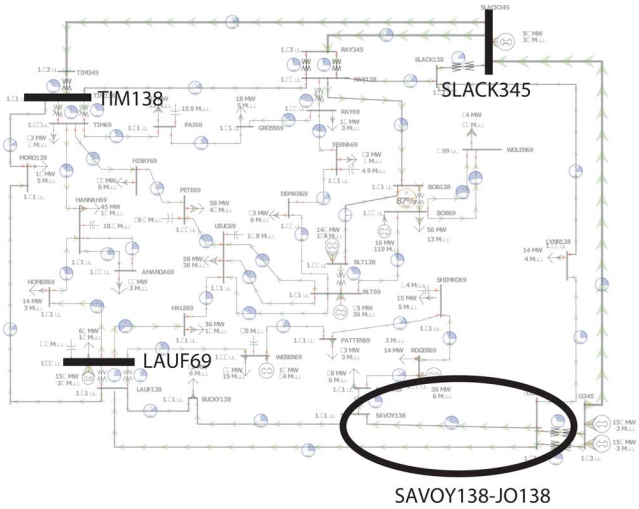

Fig. 7. PMU configuration and outage location for 37-bus test system.

A second modification is based on the observation that a line which requires a pre-outage flow exceeding the known line limit is most likely not the outaged line. For example, if the pre-outage flow on a line would have to be 100 GW in order to get the observed angle changes and the line's rating is 500 MW, that line is probably not the outaged line. Therefore, lines with pre-outage flows above a cutoff value are removed from consideration after step 3. For the examples given below, the cutoff was set to twice the line rating or 5 GW if a line limit was not known, although for a real system it is likely that these limits would be known for all lines of interest.

In addition to this refinement, the X most likely pre-outage flows calculated using (17) are presented along with line rankings. This allows the user to apply engineering judgment in deciding if pre-outage flows are reasonable. To construct the tables of results given below in the examples, X was set to five. Additional knowledge, such as known direction of flow or estimates of event locations (e.g., via FNET monitoring [31]), could also be easily incorporated into the algorithm by modification of the considered event set.

V. Examples

In order to gauge the effectiveness of our algorithm, the algorithm was tested on two systems—a 37-bus study system and the Tennessee Valley Authority (TVA) control area—with simulated and real data, respectively.

A. The 37-Bus Study System Simulated Outage

To ascertain the ability of the algorithm to correctly detect and identify line outages, the algorithm was tested using a 37-bus, nine-generator system with an average R/X ratio of 0.378 taken from [32, Ex. 13.9]. The generators were modeled as round rotor machines with quadratic saturation using an IEEE Type 1 exciter. A oneline diagram of the system is provided in Fig. 6. To examine the performance of the algorithm, dynamic simulations were run using PowerWorld Simulator to simulate the PMU data that would be obtained after the outage of the SAVOY138-JO138 line, indicated in Fig. 7. Before the outage, the power flow on the line is 73 MW from JO138 to SAVOY138.

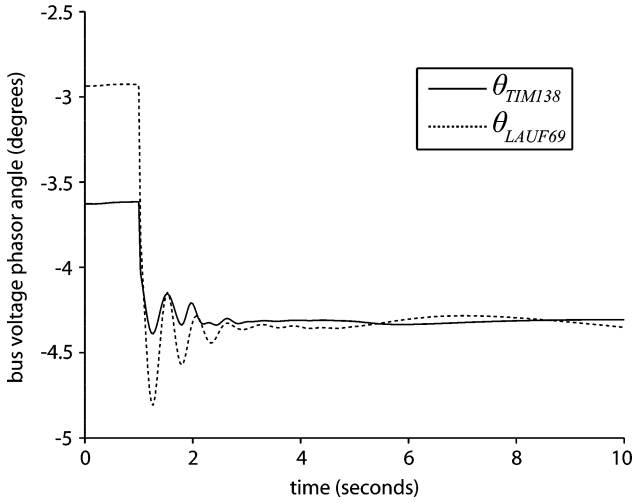

Fig. 8. Simulated angle measurements for the 37-bus system outage referenced to SLACK345 angle.

The system was simulated with PMUs located at buses TIM138, SLACK345, and LAUF69 (see Fig. 7). The simulated phasor angles at the TIM138 and LAUF69 buses, with SLACK345 used as the reference bus, are shown in Fig. 8.

Table I shows the results of running the algorithm with these bus angle measurements. The correct line is detected, and the calculated pre-outage flow on the line is only 5% away from the correct pre-outage flow value. Also, the NAD value for the correct line is 0.003, whereas the line ranked second has a much greater NAD value (0.023). Therefore, with only three PMUs on a 37-bus system, the algorithm accurately detects the line outage.

The angle values used in determining Table I were taken directly from the dynamic simulation without any noise added to the signal. To see the effects of noise on the algorithm, zero mean Gaussian noise with a standard deviation of 0.1 degrees was added to the simulated phasor angles. The angle measurements obtained are shown in Fig. 9, and the results of running the algorithm with these measurements are given in Table II. The difference between the calculated pre-outage flow value and the

TABLE I
THE 37-BUS SYSTEM RESULTS USING SIMULATED MEASUREMENTS

Rank	Line	Pre-outage flow (MW)	*NAD*
1	JO138-SAVOY138	69	0.003
2	RAY138-BOB138	90	0.023
3	BOB138-BLT138	247	0.023
4	BLT138-BLT69	247	0.023
5	JO138-LAUF138	80	0.036

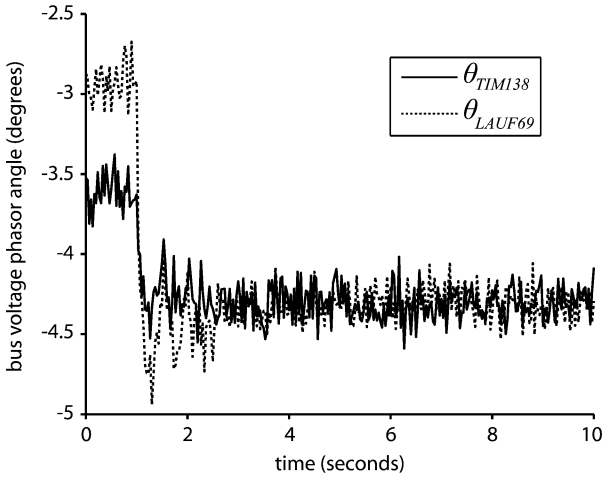

Fig. 9. Simulated angle measurements for the 37-bus system with noise added referenced to SLACK345 angle.

TABLE II
THE 37-BUS SYSTEM RESULTS WITH GAUSSIAN NOISE ADDED TO MEASUREMENTS

Rank	Line	Pre-outage flow (MW)	*NAD*
1	JO138-SAVOY138	71	0.013
2	RAY138-BOB138	92	0.033
3	BOB138-BLT138	253	0.033
4	BLT138-BLT69	253	0.033
5	JO138-LAUF138	82	0.046

correct value is 3% for the results based on the noisy measurements, which is an improvement over the noiseless measurement result. One possible explanation for this is that the addition of Gaussian noise cancels out some of the oscillations. The NAD value, however, has gone up significantly, from 0.003 to 0.013. This is still a low value, but it does show that the presence of noise in the angle measurements can have a negative impact on the estimation of the steady state angle differences and result in a higher NAD value.

B. TVA 500-kV Line Outage With Real PMU Data

The following example details the performance of the algorithm using real PMU data during a line outage in the TVA control area, with a system model consisting of 7013 buses. Real data are being shown in this example; however, due to data confidentiality issues, detailed bus and line information is not provided.

A state estimator case file was used to construct the $\mathbf{B}$ matrix. The event analyzed in this example is the outage of a 500-kV line carrying (according to the state estimator case) 1072 MW.

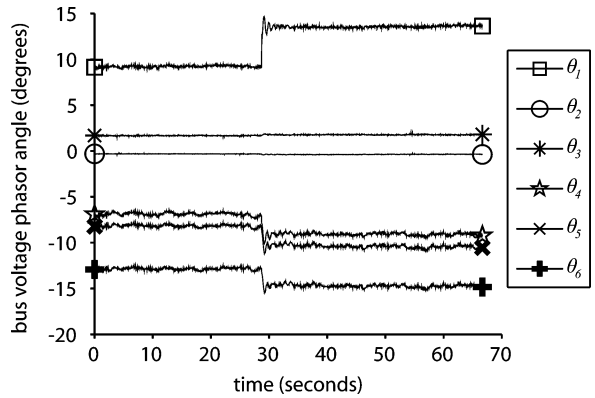

Fig. 10. PMU angle measurements on the TVA system before and after the line outage.

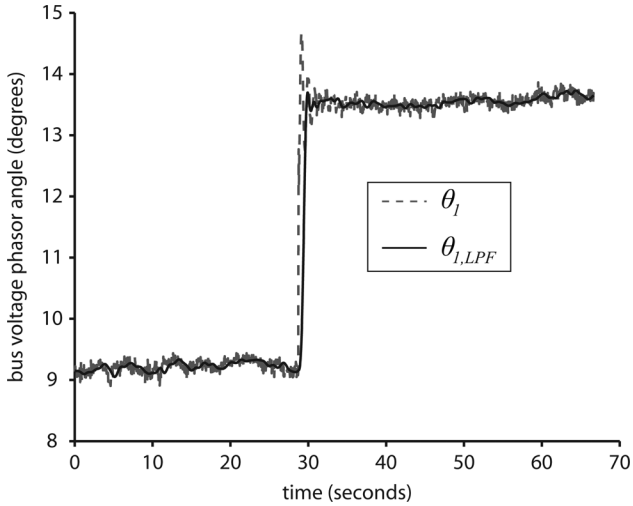

Fig. 11. Effect of low-pass filtering on real phasor angle measurements.

On the system, there were seven PMUs deployed, each providing data at 30 samples per second. One of the buses for which PMU data was available was chosen as the reference bus. The angle measurements from the other buses were then subtracted from the reference bus angles.

Fig. 10 shows the referenced PMU angle measurements before and after the line outage. Clearly, there is a significant steady state angle change in several of the PMU measurements, particularly for θ_1, θ_4, θ_5, and θ_6. Also, note that there are oscillations and noise in all of the angle measurements. However, once the low-pass filter described in the above section is applied, much of the noise and oscillations are removed. As an example, Fig. 11 shows how low-pass filtering attenuates both the noise and low frequency oscillations in the angle measurements θ_1.

Using the procedure given in (3), $\boldsymbol{\Delta\theta}_{observed}$ was calculated and the following values were obtained:

$$\boldsymbol{\Delta\theta}_{\text{observed}} = \begin{bmatrix} \Delta\theta_1 \\ \Delta\theta_2 \\ \Delta\theta_3 \\ \Delta\theta_4 \\ \Delta\theta_5 \\ \Delta\theta_6 \end{bmatrix} = \begin{bmatrix} 4.55^\circ \\ -0.06^\circ \\ 0.12^\circ \\ -2.24^\circ \\ -2.11^\circ \\ -1.90^\circ \end{bmatrix}. \tag{19}$$

TABLE III
ALGORITHM RESULTS FOR TVA SYSTEM LINE OUTAGE

Rank	Line ID	Pre-outage flow (MW)	*NAD*
1	1466	1058	0.015
2	4801	2722	0.311
3	1708	1087	0.524
4	3118	4870	0.570
5	1625	891	0.630

TABLE IV
ALGORITHM RESULTS FOR TVA SYSTEM LINE OUTAGE WITH TERMINAL ANGLE MEASUREMENT θ_1 REMOVED

Rank	Line ID	Pre-outage flow (MW)	*NAD*
1	1466	1082	0.013
2	1685	750	0.033
3	2622	4703	0.038
4	2614	4769	0.038
5	1684	1084	0.066

After $\boldsymbol{\Delta\theta}_{\text{observed}}$ was determined, the algorithm was run to predict the outaged line along with the pre-outage flow. The results from the algorithm are shown in Table III. The algorithm correctly determines the outaged line from the full set of 7013 possibilities, referred to by the identifier 1466. Also, the pre-outage flow calculated by the algorithm, 1058 MW, is only 1% different from the state estimator value of 1072 MW. Another key feature of the results shown is that the NAD value for the correct line, 0.015, is significantly lower than the 0.311 NAD value for the line ranked second.

Because one of the angle measurements, θ_1, is taken from a terminal bus of the outaged line, it is also interesting to see how the algorithm performs when this angle measurement is removed. With this angle removed, $\boldsymbol{\Delta\theta}_{observed}$ was determined to be

$$\boldsymbol{\Delta\theta}_{\text{observed}} = \begin{bmatrix} \Delta\theta_2 \\ \Delta\theta_3 \\ \Delta\theta_4 \\ \Delta\theta_5 \\ \Delta\theta_6 \end{bmatrix} = \begin{bmatrix} -0.06^\circ \\ 0.13^\circ \\ -2.29^\circ \\ -2.21^\circ \\ -1.99^\circ \end{bmatrix}. \tag{20}$$

As shown in Table IV, the algorithm still correctly detects the outaged line and determines the pre-outage flow with only a 1% difference from the state estimator flow value on the line. The main difference between the results in Tables III and IV is that the differentiation between the NAD values of the correct line and the line ranked second is much smaller in Table IV. This indicates that increasing the PMU information available allows for better differentiation between outaged lines. One other point of interest is that the line with identifier 1685 shares a bus with the correctly outaged line; therefore, if these results were visualized on a one-line display, the method presented here would still be a useful indicator of where the outage occurred in the system even if the rankings were switched.

VI. CONCLUSIONS AND FUTURE WORK

The satisfactory performance of the algorithm with both real data and simulated data on large and small power systems indicates that it is possible to use PMU data, even when coverage is extremely limited, to detect single line outage events. The results also indicate that knowledge of topology changes outside of the local control area could be obtained by using data which is currently available on the North American power grid. In addition, the presence of measurement noise and oscillatory behavior does not have a catastrophic effect on the algorithm's performance. Therefore, this algorithm can currently provide a robust way to increase operator awareness of line statuses throughout an electric interconnection. Presentation of this information to system operators would allow them to better anticipate and react to potential problems resulting from external system changes.

As mentioned in the above section on algorithm issues, it is possible for other types of events on the system to result in similar angle changes as a single line outage. Although it is not feasible to include every possible event on the system, one useful area of future research would be the extension of the event set to include a wider array of potential events such as single generator outages and multiple line outages. We are also interested in exploring the usage of phasor magnitude and frequency data, as these data values are unused in the current event detection algorithm. Finally, because the research thus far has shown that incomplete PMU coverage can be used in event detection, we are investigating ways that limited PMU placement can be optimized in order to detect events of interest.

REFERENCES

[1] US-Canada Power System Outage Task Force, Final Report on August 14, 2003 the Blackout in the United States and Canada, 2004. [Online]. Available: https://reports.energy.gov/BlackoutFinal-Web.pdf.

[2] Steps to Establish a Real-Time Transmission Monitoring System for Transmission Owners and Operators Within the Eastern and Western Interconnections, U.S. Department of Energy and Federal Energy Regulatory Commission, 2006.

[3] A. G. Phadke, "Synchronized phasor measurements in power systems," *IEEE Comput. Appl. Power*, vol. 6, no. 2, pp. 10–15, Apr. 1993.

[4] M. Donnelly, M. Ingram, and J. R. Carroll, "Eastern interconnection phasor project," in *Proc. 39th Hawaii Int. Conf. System Sciences*, Jan. 2006, pp. 336–342.

[5] W. Jiang, V. Vittal, and G. T. Heydt, "A distributed state estimator utilizing synchronized phasor measurements," *IEEE Trans. Power Syst.*, vol. 22, pt. 2, pp. 563–571, May 2007.

[6] M. Zhou, V. A. Centeno, J. S. Thorp, and A. G. Phadke, "An alternative for including phasor measurements in state estimators," *IEEE Trans. Power Syst.*, vol. 21, no. 4, pp. 1930–1937, Nov. 2006.

[7] J. S. Thorp, A. G. Phadke, and K. J. Karimi, "Real time voltage-phasor measurements for static state estimation," *IEEE Trans. Power App. Syst.*, vol. PAS-104, pp. 3098–3106, Nov. 1985.

[8] A. P. S. Meliopoulos, G. J. Cokkinides, O. Wasynczuk, E. Coyle, C. Hoffmann, C. Nita-Rotaru, T. Downar, L. Tsoukalas, and R. Gao, "PMU data characterization and application to stability monitoring," in *Proc. 2006 IEEE Power Eng. Soc. Power Systems Conf. Expo.*, Nov. 2006, pp. 151–158.

[9] K. Sun, S. Likhate, V. Vittal, V. S. Kolluri, and S. Mandal, "An online dynamic security assessment scheme using phasor measurements and decision trees," *IEEE Trans. Power Syst.*, vol. 22, no. 4, pp. 1935–1943, Nov. 2007.

[10] A. R. Khatib, R. F. Nuqui, M. R. Ingram, and A. G. Phadke, "Real-time estimation of security from voltage collapse using synchronized phasor measurements," in *Proc. IEEE Power Eng. Soc. General Meeting*, Jun. 2004, vol. 1, pp. 582–588.

[11] G. Zhang, P. Hirsch, and S. Lee, "Wide area frequency visualization using smart client technology," in *Proc. IEEE Power Eng. Soc. General Meeting*, Jun. 2007, pp. 1–8.

[12] R. Klump, R. E. Wilson, and K. E. Martin, "Visualizing real-time security threats using hybrid SCADA/PMU measurement displays," in *Proc. 38th Hawaii Int. Conf. System Sciences*, Jan. 2005.

[13] S. Chun-Lien and J. Bo-Yuan, "Visualization of large-scale power system operations using phasor measurements," in *Proc. Int. Conf. Power Systems Technology*, Oct. 2006.

[14] A. Monticelli, "Modeling circuit breakers in weighted least squares state estimation," *IEEE Trans. Power Syst.*, vol. 8, no. 3, pp. 1143–1149, Aug. 1993.
[15] A. Monticelli, "Electric power system state estimation," *Proc. IEEE*, vol. 88, no. 2, pp. 262–282, Feb. 2000.
[16] M. Kezunovic, "Monitoring of power system topology in real-time," in *Proc. 39th Hawaii Int. Conf. System Sciences*, Jan. 2006.
[17] A. Abur, H. Kim, and M. Çelik, "Identifying the unknown circuit breaker statuses in power networks," *IEEE Trans. Power Syst.*, vol. 10, no. 4, pp. 2029–2037, Nov. 1995.
[18] E. Lourenço, A. Costa, K. Clements, and R. Cernev, "A topology error identification method directly based on collinearity tests," *IEEE Trans. Power Syst.*, vol. 21, no. 4, pp. 1920–1929, Nov. 2006.
[19] US-Canada Power System Outage Task Force, Final Report on August 14, 2003 the Blackout in the United States and Canada, 2004. [Online]. Available: https://reports.energy.gov/BlackoutFinal-Web.pdf.
[20] US-Canada Power System Outage Task Force, Final Report on the Implementation of the Task Force Recommendations, 2006. [Online]. Available: http://www.oe.energy.gov/DocumentsandMedia/Blackout-FinalImplementationReport(2).pdf.
[21] R. Yeu and P. Sauer, "Post-contingency equilibrium analysis techniques for power systems," in *Proc. 37th North American Power Symp.*, Oct. 2005, pp. 429–433.
[22] J. Hauer, N. Bhatt, K. Shah, and S. Kolluri, "Performance of 'WAMS east' in providing dynamic information for the north east blackout of August 14, 2003," in *Proc. IEEE Power Eng. Soc. General Meeting*, Jun. 2004, pp. 1685–1690.
[23] D. Forsyth and J. Ponce, *Computer Vision: A Modern Approach*. Englewood Cliffs, NJ: Prentice-Hall, 2003, pp. 176–179.
[24] *IEEE Standard for Synchrophasors for Power Systems IEEE Standard*, C37.118-2005, 2006.
[25] A. Wood and B. Wollenberg, *Power Generation, Operation, and Control*. New York: Wiley, 1984.
[26] M. Liu and G. Gross, "Role of distribution factors in congestion revenue rights applications," *IEEE Trans. Power Syst.*, vol. 19, no. 2, pp. 802–810, May 2004.
[27] H. Anton, *Elementary Linear Algebra*, 8th ed. New York: Wiley, 2000, pp. 303–312.
[28] M. Crow, *Computational Methods for Electric Power Systems*. Boca Raton, FL: CRC, 2003.
[29] R. Kaye and F. Wu, "Analysis of linearized decoupled power flow approximations for steady-state security assessment," *IEEE Trans. Circuits Syst.* , vol. 31, no. 7, pp. 623–636, Jul. 1984.
[30] T. Guler, G. Gross, and M. Liu, "Generalized line outage distribution factors," *IEEE Trans. Power Syst.*, vol. 22, no. 2, pp. 879–881, May 2007.
[31] Z. Zhian, X. Chunchun, B. Billian, Z. Li, S. Tsai, R. Conners, V. Centeno, A. Phadke, and L. Yilu, "Power system frequency monitoring network (FNET) implementation," *IEEE Trans. Power Syst.*, vol. 20, no. 4, pp. 1914–1921, Nov. 2005.
[32] J. Glover, M. Sarma, and T. Overbye, *Power System Analysis and Design*, 4th ed. Burlington, MA: Thomson Engineering, 2008.

Joseph Euzebe Tate (S'03–M'08) received the B.S. degree in electrical engineering from Louisiana Tech University, Ruston, LA, in 2003 and the M.S. and Ph.D. degrees in electrical and computer engineering from the University of Illinois at Urbana-Champaign in 2005 and 2008, respectively.

He is currently an Assistant Professor in the Department of Electrical and Computer Engineering at the University of Toronto, Toronto, ON, Canada.

Thomas J. Overbye (S'87–M'93–SM'96–F'06) received the B.S., M.S., and Ph.D. degrees in electrical engineering from the University of Wisconsin-Madison.

He is currently the Fox Family Professor of Electrical and Computer Engineering at the University of Illinois at Urbana-Champaign. He was with Madison Gas and Electric Company, Madison, WI, from 1983–1991. His current research interests include power system visualization, power system analysis, and computer applications in power systems.